J Mater Sci (2011) 46:7026–7038
DOI 10.1007/s10853-011-5671-9

Banded structure in Dual Phase steels in relation with the austenite-to-ferrite transformation mechanisms

Benoit Krebs · Lionel Germain · Alain Hazotte · Mohamed Gouné

Received: 23 March 2011 / Accepted: 30 May 2011 / Published online: 14 June 2011

Abstract New experimental data are reported relative to the development of banded structures in Mn-segregated Dual Phase steels during the austenite-to-ferrite transformation stage of their final heat treatment. Two types of ferrite are detected to grow simultaneously, i.e. allotriomorph and acicular ferrite, with distinct consequences on the topology of the final (ferrite + martensite) microstructure: allotriomorph ferrite sharpens the banded structure of ferrite and martensite between Mn-poor and Mn-enriched regions, respectively, whereas acicular ferrite favours more isotropic microstructures. Owing to an original image treatment procedure, the sharpness of banded structure is quantitatively analyzed for different heat treatment conditions. Results confirm those of previous works, but we propose to rather explain them by considering that a change in a heat treatment parameter results in a variation in the respective amounts of both ferrite types.

Introduction

The formation mechanisms of banded structures (alternating parallel bands of ferrite and pearlite or martensite) in steels are not well understood. If it is known that process parameters such as the austenitization temperature and the cooling rate have an influence on the final anisotropy of the material [1], the fundamental mechanisms are still not clear. This lack of understanding prevents future optimization of steel products by a better control of the microstructure. Indeed, banding impacts the resistance to hydrogen cracking, toughness and damage resistance [2]. This research work shows new experimental evidence and proposes mechanisms by which banding structures forms. Furthermore, it describes process parameters that could lead to a better control of microstructures.

It is well established that the bands in ferrite/pearlite microstructures are strongly related to the microsegregation of alloying elements that results of the solidification process [3, 4]. The alloying elements (Mn, Si, …) are rejected from the formed δ ferrite dendrites. This leads to a high solute content in the interdendritic regions, which is retained during the transformation from δ to γ-austenite. This solute distribution provides basis for microstructural banding. One evidence is that bands are eliminated when the microsegregation of alloying elements is removed through a specific thermal treatment.

One of the first mechanisms proposed to explain the banded microstructure formation is based on the effect of alloying elements on the carbon activity in austenite [5]. In other words, the regions in austenite with different amounts of substitutional alloying elements will lead to regions with different level of carbon. The subsequent ferritic phase transformation during cooling will be affected by this composition heterogeneity; ferrite will form preferentially in the low carbon regions whereas pearlite (or martensite) will form in the high carbon austenite regions, leading to banding microstructures. In that mechanism, the effects of nucleation or growth of ferrite are not discussed.

An alternative mechanism may indicate the importance of the ferrite nucleation process. Bastien proposed that microstructural banding is a result of the effect of

B. Krebs · L. Germain (✉) · A. Hazotte
Laboratoire d'Etude des Microstructures et de Mécanique des Matériaux (LEM3), UMR CNRS 7239, Université Paul Verlaine, Ile du Saulcy, 57045 Metz, France
e-mail: lionel.germain@univ-metz.fr

M. Gouné
ArcelorMittal Research SA, R&D Automotive Products, Voie Romaine, 57280 Maizières-lès-Metz, France

substitutional alloying elements distribution on the temperature at which ferrite forms (i.e. the Ar3 temperature) [3]. The ferrite will nucleate first in the solute poor regions where the Ar3 temperature is lowered and then in the solute rich regions where the Ar3 temperature is raised. In either case, carbon atoms, which diffuse rapidly, are rejected from ferrite to austenite regions, which finally transform to pearlite or martensite. Calculations based on thermodynamic considerations and performed by Verhoeven confirmed that variations in Mn concentration result in variations in carbon concentration which can significantly affect the local Ar3 [6]. Based on this ferrite nucleation mechanism, Kirdaldy et al. [7] proposed a semi-empirical expression for the critical cooling rate which can prevent the banding microstructure formation. More recently, Offerman et al. [8] have proposed a model to control the banding structure in steels, which suppose that the banding structure formation is mainly controlled by the difference in nucleation rates (that can be linked with the cooling rate). When it exceeds 6–8% ferrite, pearlite banding occurs. Xu et al. combined this concept with calculations of segregation due to solidification [9]. These successful applications of these models may indicate the importance of nucleation on the formation of banding.

In most of works done on that topic, the influence of the austenite-to-ferrite transformation modes has been neglected, especially to explain the effect of initial austenite grain size or the effect of cooling on the intensity of the banding structure. Indeed, a high cooling rate prevents a strong banding and an initial austenite grain size larger than the microchemical band spacing can decrease the intensity of the banding structure. Samuels [1] suggests that it could be linked to the acicular ferrite presence in the final microstructures.

In this work, we propose new experimental evidence which clearly show that the ferrite transformation mechanism cannot be ignored in order to improve our understanding on the banded structure formation. The influence of process parameters in relation with the austenite-to-ferrite transformation mode is discussed. In particular, this work allows take a fresh look at the effect of initial austenite grain size on the intensity of the banded structure in Dual Phase (DP) steels composed essentially of ferrite and martensite.

Materials and methods

Material

Table 1 reports the mean chemical composition of the steel used in the present study. The metal was available in the form of a sheet, 3 mm in width, issued from a usual industrial process involving continuous casting then hot rolling. For the purpose of the present study, parts were cold rolled down to 1.2 mm (reduction factor = 60%), then cut as small parallelepiped samples, 10 mm in length and 1.2 × 4 mm in section. As expected, these samples contained Mn-segregated bands parallel to the rolling direction. This is illustrated in Fig. 1b, which shows a Mn concentration map measured by electron microprobe. Local Mn concentrations were estimated to vary between about 1% (dark zones) and 2% (light zones).

Table 1 Nominal chemical composition (weight percent) of the steel used in this work

C	Mn	Si	P	S
0.15	1.48	0.013	0.01	27 ppm

Before room temperature rolling, one part of the sheet was cut and submitted to a homogenization heat treatment during 1 h at 1200 °C. These conditions were calculated and verified to be able to reduce Mn segregation below the detection limit of usual analysis methods [10]. This treatment was performed under vacuum, the metal surface having previously been coated with a refractory cement to avoid decarburization. In the following, samples and microstructures extracted from this part will be designed as 'homogeneous'.

Heat treatments

A set of heat treatments was given to the different—segregated or homogeneous—samples, in order to obtain Dual Phase (ferrite + martensite) microstructures. These 'DP' heat treatments were performed with a dilatometer (model DIL805 from BAHR Thermoanalyse Gmbh), under helium partial pressure (0.8 bar). This equipment allows performing controlled thermal cycles through induction heating, then quenching the sample by helium blowing. Temperature was continuously recorded by a K-thermocouple spot welded on the surface in the middle of one main face of the sample. Final microstructures were verified to be reproducible on a given section of the sample. Nevertheless, due to heat extraction by sample holders, the extremities were observed to be noticeably colder than the middle part of the sample. For that reason, dilatometry curves were not used for quantitative analysis of transformation kinetics.

Figure 2 shows a typical DP heat treatment applied to the samples. Its parameters were chosen to be representative of the industrial process, while promoting last stage of austenite-to-ferrite transformation in isothermal conditions. For all samples, heating up to the austenitic domain was performed with a rate equal to 10 °C/min. The time for

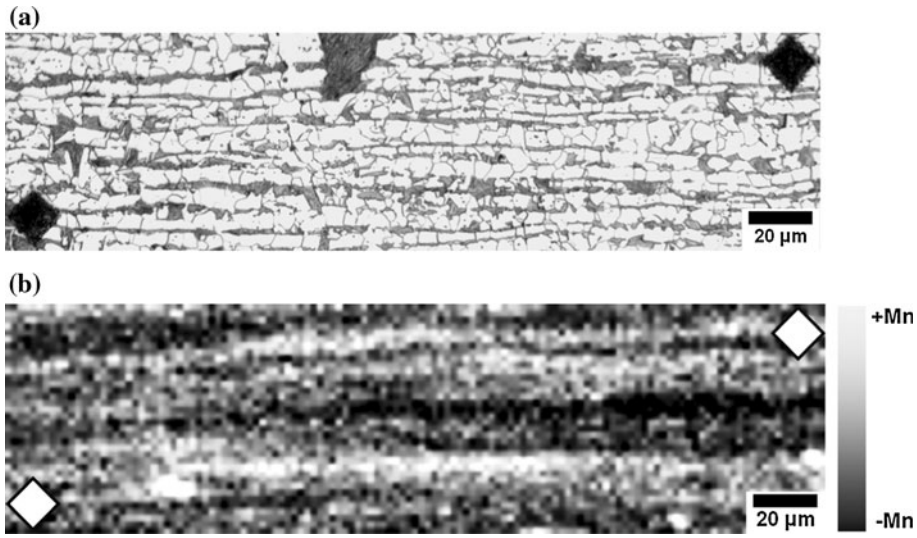

Fig. 1 **a** Optical micrograph of the banded structure obtained after a 'reference' DP heat treatment described in "Heat treatments" section (rolling direction is *horizontal*; direction normal to the sheet is *vertical*); **b** Mn concentration map measured in the same area, illustrating segregated bands resulting from the elaboration process (hardness indentations have been used to fit both surfaces)

complete austenitization at T_γ was always chosen equal to 100 s. Although different temperatures were tested for isothermal austenite-to-ferrite transformation [10], all treatments discussed in this article were given with $T_\alpha = 650$ °C. This temperature was chosen to lead to a final equilibrium austenite/martensite amount close to the values obtained with industrial processes (about 30%), while avoiding the formation of pearlite.

Different microstructures were elaborated through the variation of three main process parameters: (a) the austenitization temperature, T_γ, determining the mean austenite grain size, (b) the cooling rate from the austenitic domain, ρ_α, related to the transformation driving force and (c) the time for isothermal $\gamma \rightarrow \alpha$ transformation, t_α, leading to different volume fractions of ferrite and martensite/austenite phases. The final helium quenching promotes the transformation of the residual austenite in martensite. With regard to the quenching rate (higher than 300 °C/s), we consider that the final martensite volume fraction is equal to the fraction of austenite still present at T_α before quenching.

A large part of our results, in particular those presented in the first part of "Results" section, are related to a so-called 'reference' thermal cycle, in which T_γ and ρ_α were fixed to 870 °C and −10 °C/min, respectively.

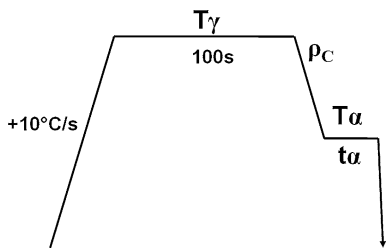

Fig. 2 Schematization of the different heat treatments performed

870 °C is the lowest temperature tested for which the austenitization was complete after 100 s; in other terms, it is the austenitization temperature which conserves the smallest austenite grain size (mean equivalent diameter around 10 µm). A cooling rate of −10 °C/min is close to the mean cooling rate observed in industrial conditions. In the case of the reference thermal cycle, the quenching was also performed at various temperatures during the cooling stage, in order to follow the austenite-to-ferrite transformation kinetics.

Characterization methods

The heat treated samples were mechanically polished up to grade 4000 diamond paste, then etched with Villela reagent (4 g picric acid and 1 ml hydrochloric acid in 100 ml ethanol) for 2–5 s at room temperature. Microstructure was observed by optical microscopy (BX61 Olympus microscope). Figure 1a gives an example of a typical banded DP structure obtained after a reference heat treatment. All the images showed hereafter were taken in the middle part of the samples (i.e. close to the thermocouple location), with their horizontal axis parallel to the rolling direction and their vertical one normal to the sheet surface.

The martensite volume fraction, $Vv(\alpha')$, was measured by a classical image analysis method, using the dedicated software Aphelion (copyright ADCIS S.A. and A.A. Imaging). Martensite was discriminated through a grey level criterion on images from optical microscopy. At least 20 images were used to estimate $Vv(\alpha')$ on a given sample.

The intensity and fineness of ferrite–martensite banded structures were also quantitatively analyzed from optical micrographs, using an original image treatment algorithm presented in details elsewhere [11]. In a few words, this method is based on the measurement of the covariogram of

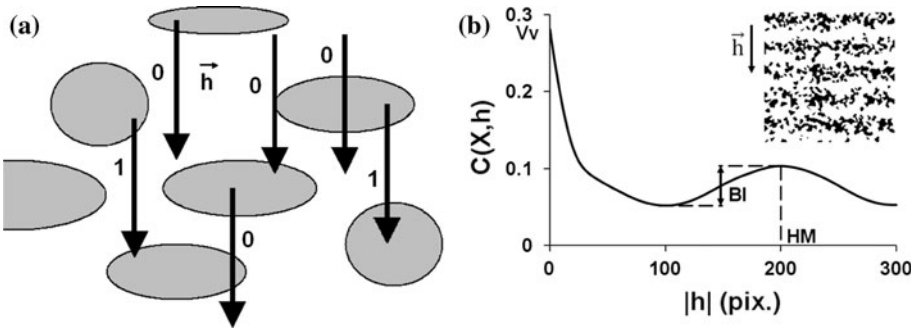

Fig. 3 **a** Illustration of the covariogram principle: among the six vectors $\vec{h}$ randomly located on the binary set, only the two counted for 1 have their extremities both belonging to the analyzed phase (*in grey*); **b** example of covariogram measured on a model binary image presenting periodicity along the direction of vector $\vec{h}$ (see [11] for details)

martensite. The covariogram is the curve reporting the probability that both extremities of a vector $\vec{h}$ belong to the analyzed phase, as a function of $\vec{h}$ modulus (see Fig. 3a for an illustration of the principle and Refs. [11–13] for more details). If the analyzed phase presents a periodicity along $\vec{h}$ direction, its covariogram will show oscillations. One example is given in Fig. 3b. Covariograms perpendicular to the rolling direction were automatically acquired using a dedicated image analysis program. Then, the height of the first oscillation was measured as the quantitative parameter to characterize the intensity of banded structures. This parameter, noted BI (for 'band intensity'), is defined on Fig. 3b. Its value varies between 0.005 that corresponds to an isotropic microstructure[1] and 0.05 that corresponds to a strongly banded one [11]. The value of $\vec{h}$ modulus corresponding to the first maximum, noted HM, is used as an estimator of the mean distance between bands. Measures were performed on at least 20 microstructures and results given hereafter indicate the average values of BI and HM with standard deviation as error bars.

High resolution Electron Back Scatter Diffraction (EBSD) was used to determine the crystallographic orientations in the microstructure. The principle and interest of this technique have been detailed in several books or articles (see for instance [14]) and will therefore not be discussed here. Since efficient phase identification and orientation indexation require working on a perfectly flat and stress-relaxed surface, an additive polishing with OPS was performed, without any additive etching. EBSD analysis was performed on a 6500F scanning electron microscope equipped with a field emission gun (FEG-SEM JEOL F 6500), with the EBSD camera Nordlys S from Oxford (HKL). Although both ferrite and martensite phases were identified as cubic phases, they can be discriminated from the difference of sharpness between their respective Kikuchi patterns ('Band Contrast'). One example of a 'Band Contrast image' is represented in Fig. 4.

Results

Kinetics and mechanisms of austenite-to-ferrite transformation

Figures 5 and 6 show micrographs collected from segregated samples quenched at different stages of the reference thermal cycle, during cooling and isothermal steps, respectively. The micrograph of one homogeneous sample quenched during isothermal step has also been added in Fig. 6b for comparison with Fig. 6c. Figure 7 reports the evolution of martensite (i.e. austenite) volume fraction Vv(α') as well as of band intensity factor (BI) as a function of time during the cooling and isothermal steps, for both segregated and homogeneous samples. For the tested cooling rate (−10 °C/min), austenite-to-ferrite transformation takes place already during the cooling step: more

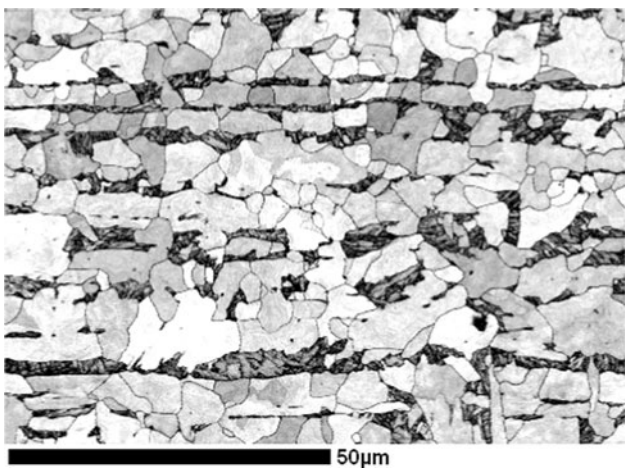

Fig. 4 Banded structure as visualized by EBSD mapping ('Band Contrast image')

[1] Note that, in the case of a homogeneous microstructure, BI factor is very low but never equal to zero; a smooth oscillation is still observed, associated with a non-random distribution of ferrite and martensite grains. In that case, HM values are not associated with band periodicity, but with the mean size of the elementary cell representative of the two phase structure.

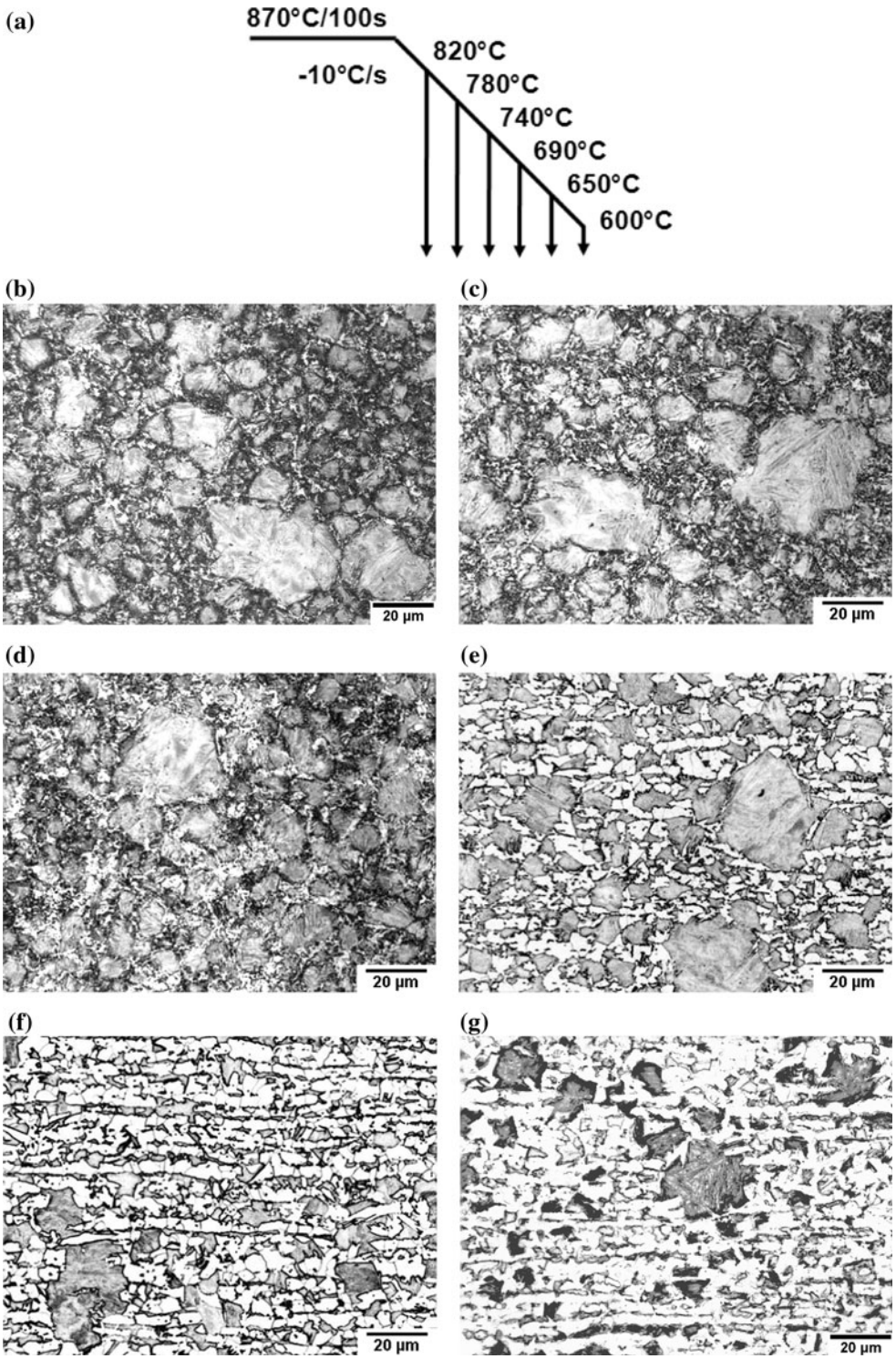

Fig. 5 Microstructures of segregated samples quenched from different temperatures (from 820 to 600 °C for **b–g** micrographs) during the continuous cooling step of the reference thermal cycle as schematized in **a**

than 50% of austenite is already transformed at 650 °C. The development of segregated bands is confirmed to be associated with Mn segregation, since the chemically homogenized samples clearly show a homogeneous DP structure in the same heat treatment conditions. The anisotropy rather appears to develop below 700 °C, and mostly during the earlier time of isothermal step. This can be clearly observed on the micrographs. This is also evidenced by the evolution of BI factor which is still close to the one measured on homogeneous samples at the end of cooling and at the beginning of isothermal step. Then BI increases rapidly during the isothermal stage. These results suggest that the banded structure development should be related to the ferrite growth rather than to its nucleation.

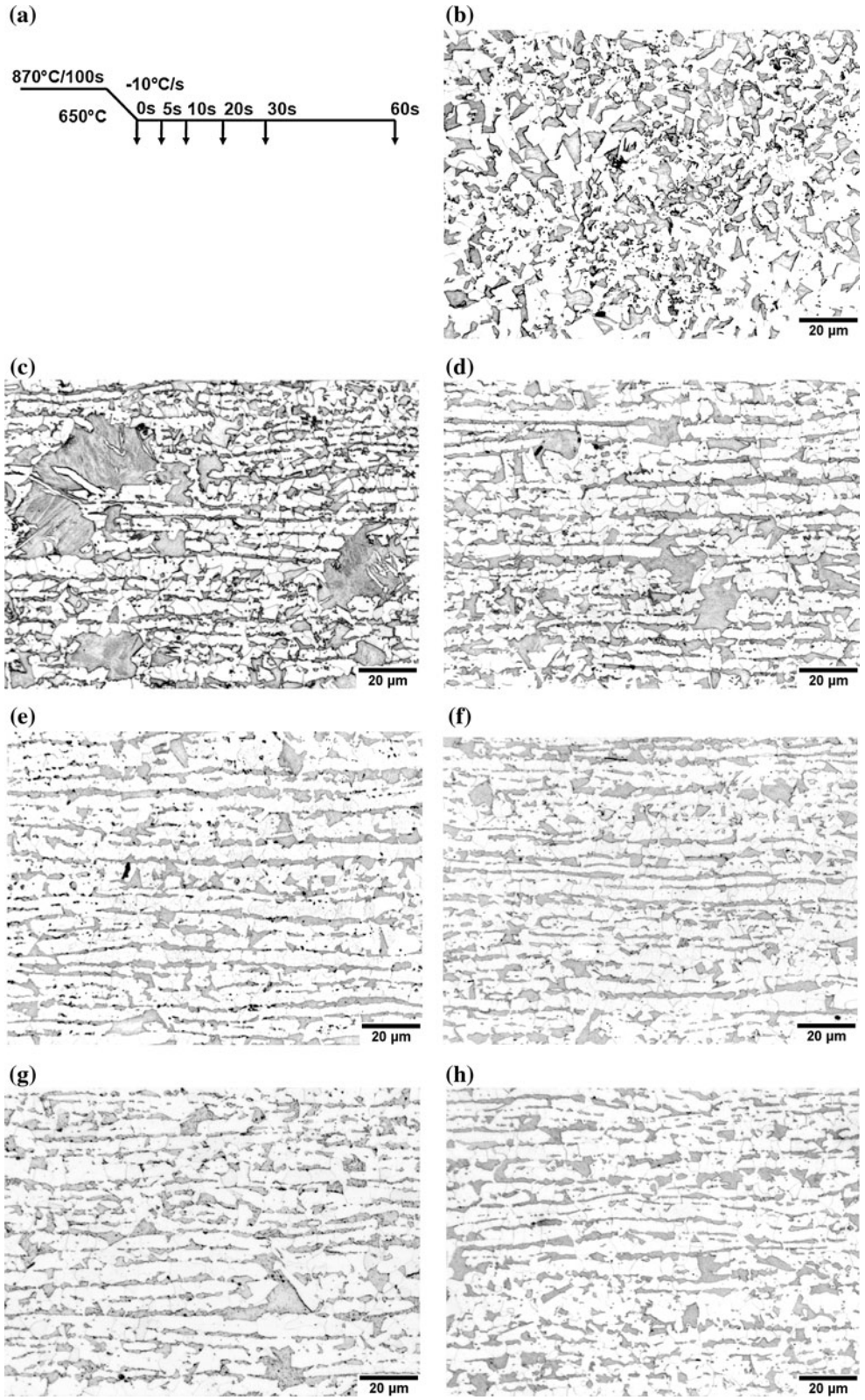

Fig. 6 Microstructures obtained after quenching at different times during the last isothermal step of the reference thermal cycle; **a** schematization of the heat treatment; **b** homogeneous sample treated for 0 s at 650 °C; **c**–**h** segregated samples treated for 0 s (**c**), 5 s (**d**), 10 s (**e**), 20 s (**f**) and 60 s (**g**)

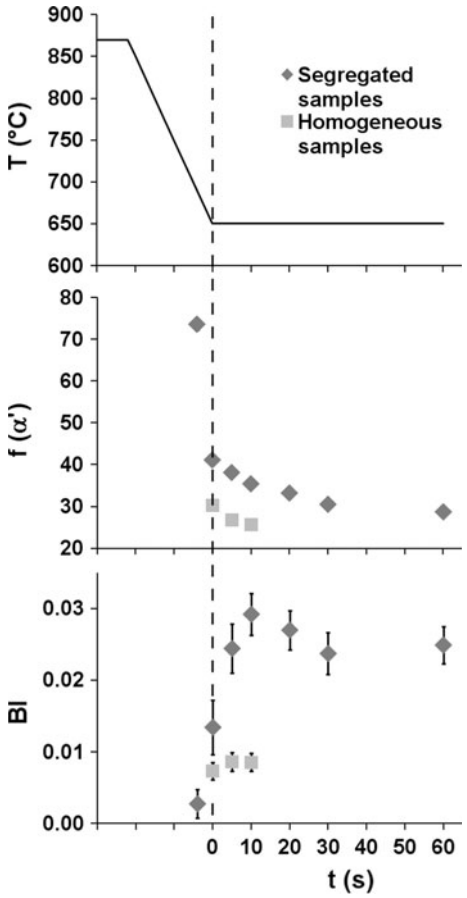

Fig. 7 Evolution of the martensite/austenite volume fraction and of the band intensity factor, BI, as a function of the time during the cooling and the last isothermal step for both segregated and homogeneous samples

More precisely, it is observed to take place by progressive splitting of large austenite grains by growing ferrite grains, as it is particularly detectable on micrographs Fig. 6c and d.

In order to understand the way ferrite develops to the detriment of segregated austenite grains, high resolution EBSD scans were performed on several prior austenite grains visually identified to encounter a fragmentation process. Two typical examples of our observations are given in Fig. 8. Figure 8a and b show band contrast maps obtained in two samples quenched during isothermal step of the reference thermal cycle. Figure 8c and d report the corresponding {100} pole figures, collecting the orientations of all pixels included within the outline of the ex-austenitic grain. Martensite is well known to form from the austenite by following the orientation relationship of Kurdjumow–Sachs (K–S) [15]. Then using the approach proposed by Humbert et al. [16], one can calculate and plot the theoretical orientations that are related to an austenite grain by the K–S relationship. These are indicated in Fig. 8e and f. These particular orientations are expected to be those of all martensite needles formed during the quenching from the residual part of the prior austenite grain. In counterpart, dots which are far from these orientations correspond to grains which are not in K–S relationship with the prior austenite grain.

Our crystallographic analyses clearly pointed out two types of ferrite developing within austenitic grains. The first one, illustrated by Fig. 8a, c and e shows no particular crystallographic orientation relationship with austenite grain ('host' γ grain). It is also characterized by a rather smooth convex shape. The growth of this ferrite appears to be strongly oriented by the presence of Mn segregation. Indeed, as it can be seen on micrograph Fig. 8a, α grains elongate along the direction of Mn segregation bands, which results in a splitting of the host γ grain. In the following, we will denote this type 'allotriomorph ferrite'. Indeed, we consider that its development should be driven by the mechanism, described in literature, which involves ferrite grains nucleation at γ/γ grain boundaries, in orientation relationship with one of their neighbour γ grains ('parent' grain), then growth in the other γ grain (host grain) without any relationship with it. The second type of ferrite detected in the treated samples is illustrated on Fig. 8b, d and f. This ferrite clearly shows a crystallographic orientation relationship with its host γ grain and presents an acicular morphology. In addition, its development seems to be not so dependent on the presence of Mn segregation, as it can be seen on Fig. 8b. This type will be denoted 'acicular ferrite' in the following.[2] It is worthwhile to note that both types of ferrite were observed in samples submitted to the reference thermal cycle. Unfortunately, their respective proportions are difficult to estimate. Indeed, their identification requires the knowledge of prior austenite grain boundaries, which is difficult in the last stage of the transformation process when most austenite has been already transformed.

From these observations, it clearly appears that two types of austenite-to-ferrite transformation mechanisms—i.e. allotriomorph and acicular—occur during the final heat treatment of DP steels. From the point of view of the exacerbation of Mn segregation through the development of banded structures, these two modes are not expected to act similarly. The allotriomorph ferrite preferentially develops along the Mn-depleted regions. This results in a fragmentation of the austenite grains along the direction of Mn segregation, thus in a sharpening of the segregated bands. At the opposite, the acicular ferrite appears to develop in more random directions, which result in a less banded microstructure.

[2] In this study, no discrimination is made between acicular ferrite and Widmanstätten ferrite, since both present same morphology and orientation relationship.

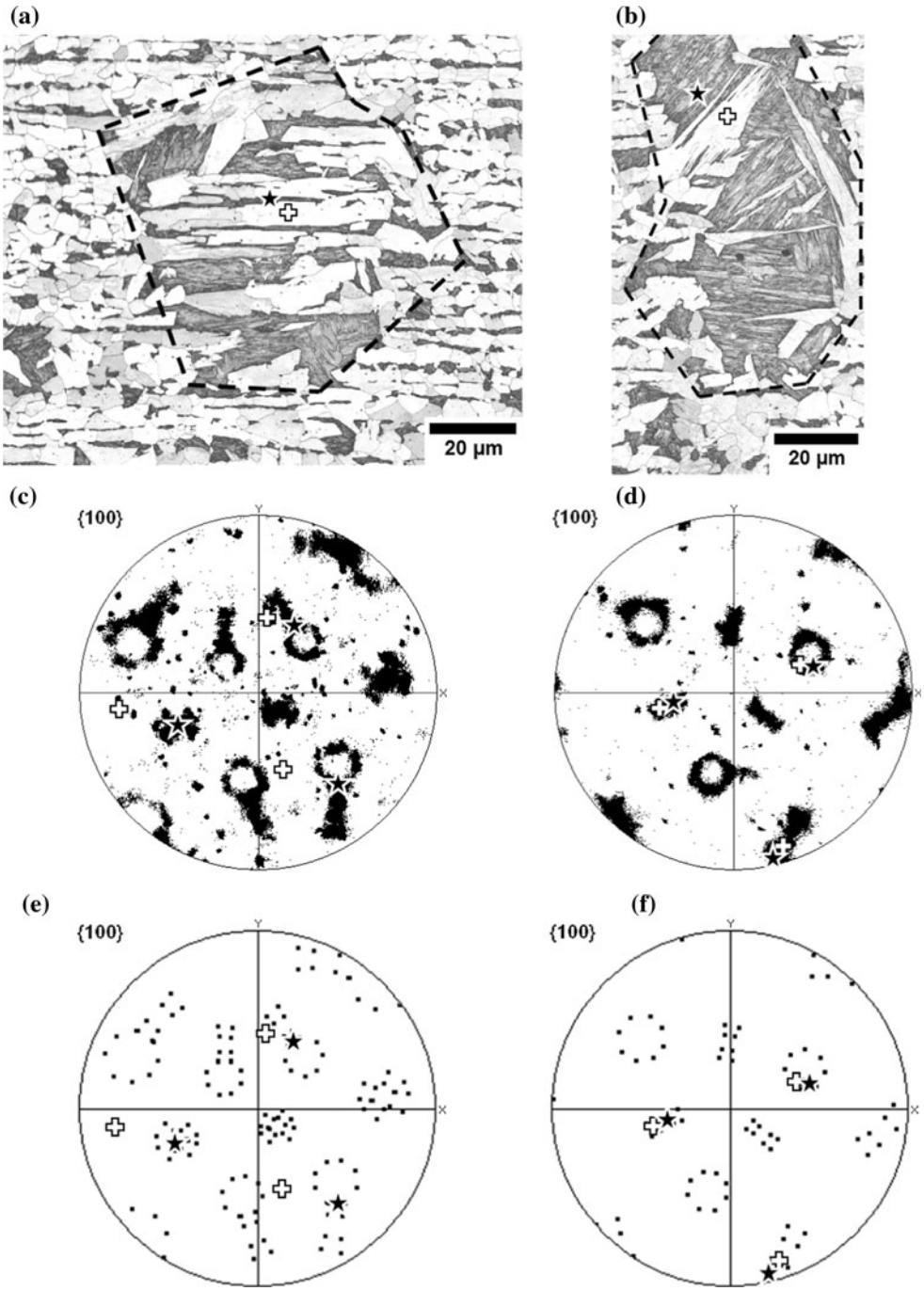

Fig. 8 **a**, **b** Two EBSD 'band-contrast' images from samples quenched during isothermal step of the reference thermal cycle; **c**, **d** associated pole figures: *dots* correspond to the orientations of every pixel in zones outlined in **a** and **b** maps; **e** and **f** theoretical orientations of the grain having a KS orientation relationship with the prior γ grain. *Black stars* and *white crosses dots* gives the orientation of particular ferritic and martensitic phase, respectively

With regard to our microstructure characterization procedure, a sharpener band structure is associated with a higher value of the band intensity factor, BI. In the following, we will conversely assume that high BI values could also point out the preeminence of the allotriomorph ferrite development mode. To strictly prove this assumption would require a quantitative analysis of the volume fraction of both type of ferrite discriminated on a misorientation-with-host grain criterion, which is unfortunately not feasible at the present time. Our direct observations of the microstructure features confirmed this working hypothesis: the lower the BI is, the higher the acicular ferrite fraction appears.

Influence of processing conditions on the development of segregated band

This part will focus on the influence of the heat treatment parameters on the final microstructure. This will be achieved by successively modifying some parameters of the reference heat treatment, then by analyzing the consequences on the microstructures, which will be

quantitatively analyzed through the procedures presented in "Materials and methods" section.

Influence of the cooling rate from austenite domain

Figure 9 shows several microstructures of homogeneous (b) and segregated samples (c–f) isothermally transformed after cooling at different cooling rates ρ_c ranging from −5 to −100 °C/s. Figure 10 reports the corresponding values of the band intensity parameter (BI; a) and of the mean distance between bands (HM; b). For a given initial Mn segregation and austenite grain size, it is clearly seen that the higher the cooling rate is, i.e. the higher the driving force for γ to α transformation, the less pronounced the final banded structure is. This becomes particularly obvious when using BI factor to quantify anisotropy: Fig. 10a

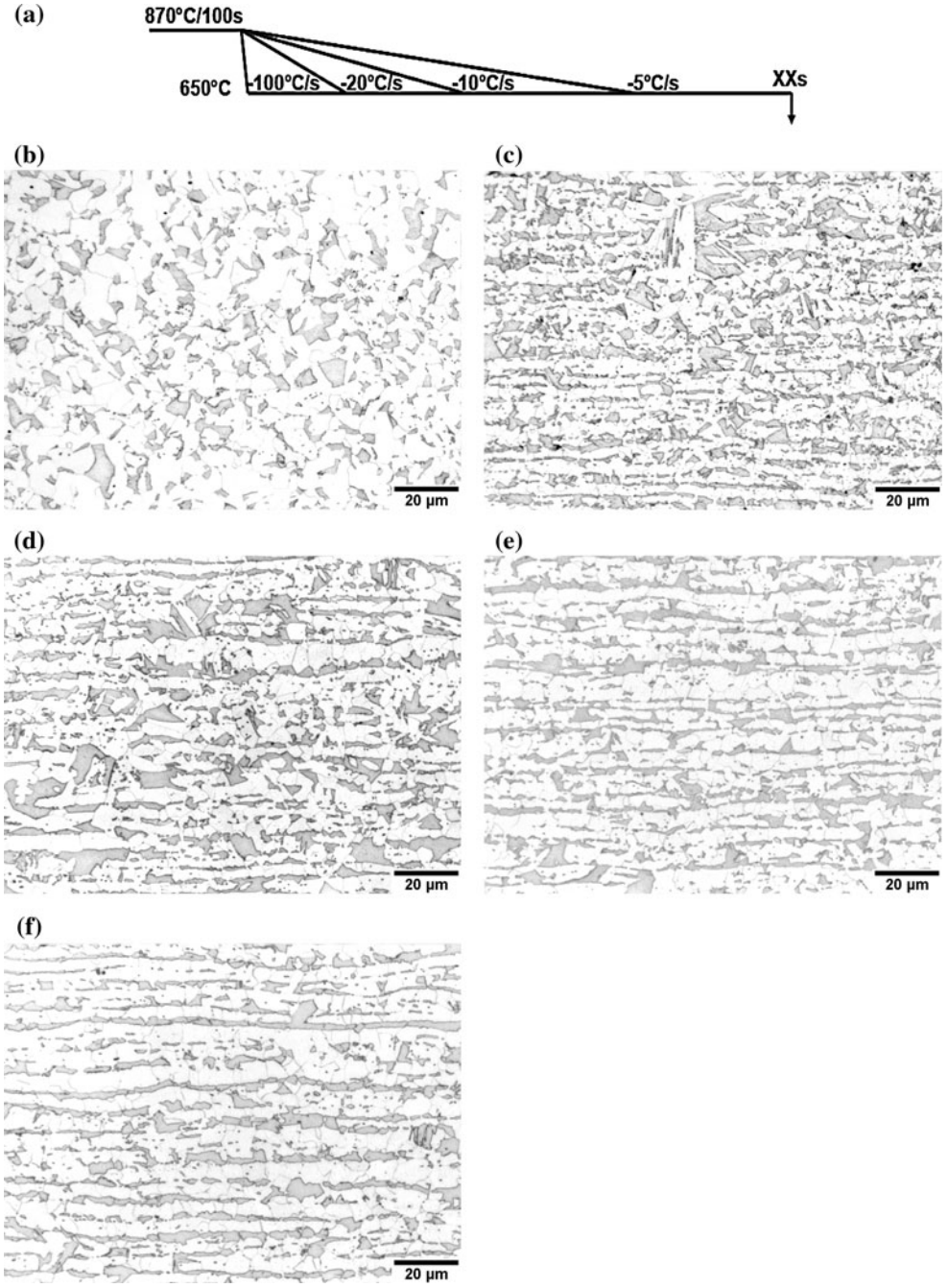

Fig. 9 Microstructures resulting from the different heat treatments schematized in **a** and corresponding to **b** homogeneous sample treated with cooling rate $\rho_\alpha = -10$ °C/s and time for isothermal transformation $t_\alpha = 5$ s; **c–f** segregated samples treated with **c** $\rho_\alpha = -100$ °C/s, $t_\alpha = 60$ s; **d** $\rho_\alpha = -20$ °C/s, $t_\alpha = 40$ s; **e** $\rho_\alpha = -10$ °C/s, $t_\alpha = 20$ s and **f** $\rho_\alpha = -5$ °C/s, $t_\alpha = 20$ s

shows a continuous decrease of BI values with increasing cooling rate, although values corresponding to an isotropic microstructure (homogeneous sample) cannot be reached even with the highest cooling rate used in this study. Figure 10b also points out that the refinement of the band structure seems to slightly increase with increasing cooling rate, at least for cooling rates ranging between −5 and −20 °C/s.

Influence of the initial austenite grain size

Figure 11 collects microstructures from segregated samples heat treated with the same cooling rate, $\rho_\alpha = -10$ °C/s, and same time for isothermal transformation, $t_\alpha = 60$ s, but starting from three different austenitization temperatures, i.e. three different initial austenite grain sizes. Figure 12 reports the values of BI (a) and HM (b) parameters measured after these three DP heat treatments. Although the trend appears not so clearly as for the effect of cooling rate, it can be seen that a higher austenitization temperature, i.e. a larger mean grain size, results in a less pronounced banded structure (Fig. 12a). More unexpectedly, the initial grain size also appears to influence the inter-band spacing of the final band structure (Fig. 12b), although the austenitization time used (100 s) is not expected to noticeably affect Mn segregation, even for the highest temperature used.

Note that in the frame of this work, we also performed some DP heat treatments in which a short plateau at 870 °C was inserted between austenitization at different temperatures and continuous cooling [10]. Their results will not be presented in the present paper for shortness purpose, but they showed similar trends as the ones illustrated here. More generally, a large set of experiments was performed for coupling the influence of T_γ, ρ_c and T_α (see Fig. 2 for definitions). Microstructure observation and quantification

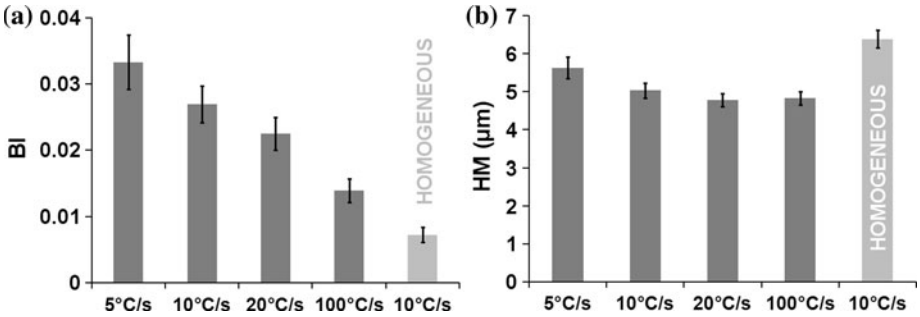

Fig. 10 Evolution of the band intensity factor (BI; **a**) and mean distance between bands (HM; **b**) as a function of the cooling rate, for both initially segregated and homogeneous samples

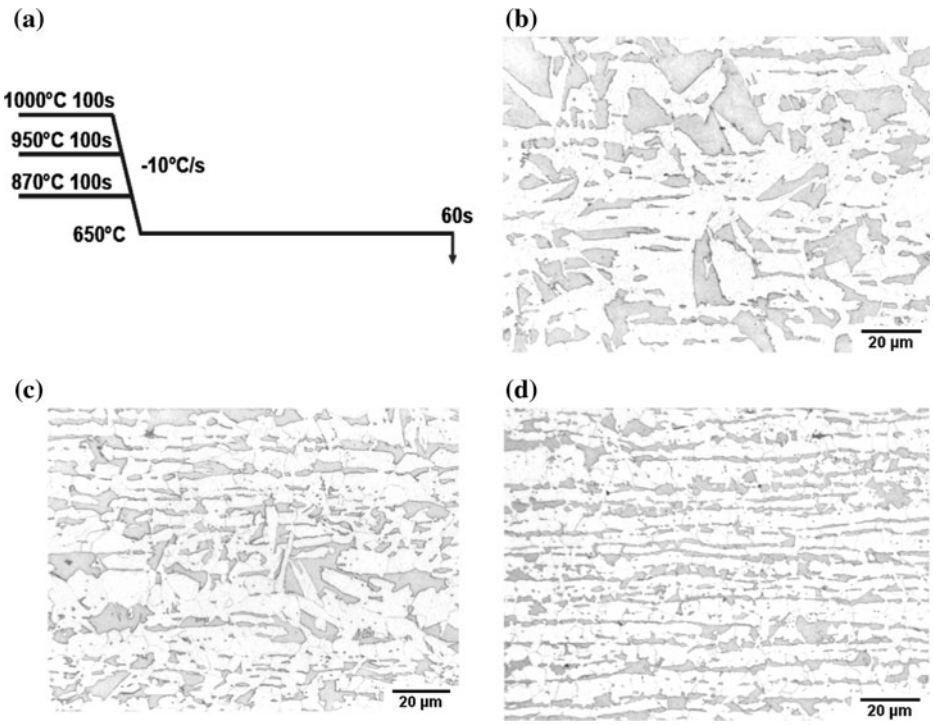

Fig. 11 Microstructures resulting from DP heat treatments schematized in **a** using the same cooling rate $\rho_\alpha = -10$ °C/s and the same time for isothermal transformation $t_\alpha = 60$ s, but starting from different austenitization temperatures: **b** 1000 °C, **c** 950 °C and **d** 870 °C

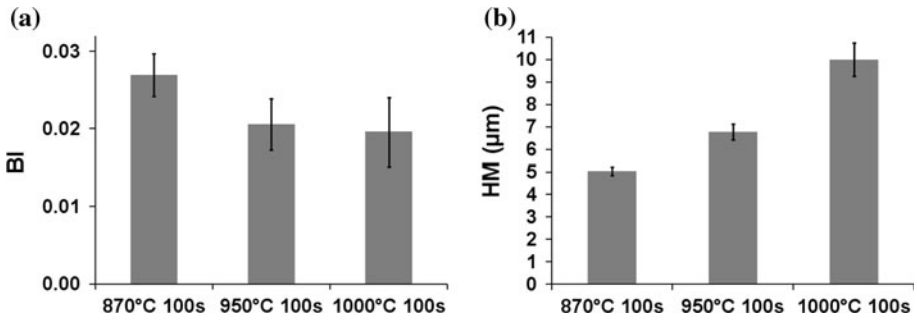

Fig. 12 Evolution of the band intensity factor (BI; **a**) and mean distance between bands (HM; **b**) as a function of austenitization temperature

showed that the anisotropy of banded structure can be reduced by increasing the austenitization temperature and/or increasing the cooling rate and/or decreasing the temperature for isothermal transformation.

Discussion

The transformation of austenite-to-ferrite during cooling is one of the most studied topics in physical metallurgy but it still remains not well understood [17, 18]. Some aspects are often discussed and lead to controversies. The experiments performed in that paper coupled with the analysis of the BI index evolutions clearly show the influence of cooling rate and initial austenite grain size on the formation of banded structure in DP steels. The banded structure is less pronounced when the cooling rate is higher and when the initial austenite grain size is larger. These results are summarized in Fig. 13. They confirm the works done by Samuels [1] and Thompson and Howell [4] who concluded that a high cooling rate prevents a strong banding and that an initial austenite grain size larger than the microchemical band spacing can decrease the intensity of the banding structure. The proposed mechanism for such behaviour is double. They supposed that the banding structure is mainly controlled by the difference in ferrite nucleation rate in the Mn poor and rich regions, which also depends on the cooling rate. When the cooling rate is higher, the difference in ferrite nucleation is lower. Therefore, the probability for ferrite to nucleate in both regions is higher. As a result, the banding structure is less intense. Furthermore, the banding structure becomes less pronounced when the initial austenite grain size is two or three times larger than the inter-segregation spacing [1, 2]. Therefore, another possible mechanism was proposed from the work done by Grosterlinden et al. [2]. It is founded on two considerations. The first one is that each austenite grain boundary intercepts at least one Mn rich region. The second one is that ferrite nucleates and growths rapidly along the austenite grain boundaries since the diffusivity of carbon can be four order of magnitude higher than bulk diffusivity. As a consequence, the banding structure can be broken and reduced for the main reason that the ferrite can grow within the Mn rich region through the austenite grain boundaries.

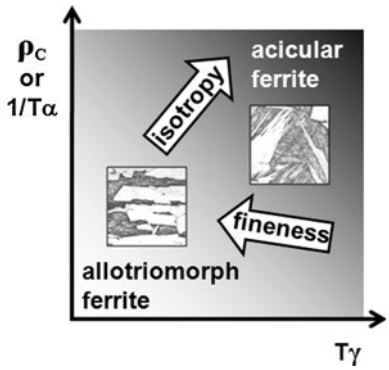

Fig. 13 Synthesis of the main results obtained in the present work

Our observations and measurements on the effects of both cooling rate and initial austenite grain size on banding structure formation are clearly in agreement with those coming from [1, 2]. Nevertheless, they lead to propose a mechanism that differs radically from theirs and from those published in that field.

Firstly, nucleation and growth stage were decoupled by using a cooling rate of −10 °C/s and the BI evolution clearly shows an increase of banding during isothermal treatment at 650 °C. These results suggest that development of segregated bands should be related to the growth of ferrite rather than to its nucleation.

Furthermore, our observations clearly showed that two types of ferrite—i.e. allotriomorph and acicular—are formed during the holding at a given temperature. The two transformation mechanisms involved act differently on the banding structure. Indeed, allotriomorph ferrite growths preferentially along the Mn poor regions and accentuates the banded structure. Acicular ferrite develops in more random directions from the austenite grain boundaries, resulting in a more isotropic microstructure. Therefore, the austenite-to-ferrite transformation type affects the microstructure topology and the intensity of the banded structure. The proposed mechanism is supported by the effect of cooling rate and initial austenite grain size on the banded structure formation. There have been many studies about

the occurrence of acicular ferrite (or Widmanstätten ferrite) in steels as a function of chemical composition, austenite grain size and cooling rate [19–22]. It is well established that acicular ferrite is favoured by a large austenite grain size. In that situation, the growth of allotriomorph ferrite is firstly favoured along the austenite grain boundaries and subsequently acicular ferrite forms as secondary plates growing from allotriomoph ferrite layers. This is probably the main reason why acicular ferrite is rarely found in isolation. When the austenite grain size is small, the formation of allotriomorph ferrite is favoured, its growth is more isotropic and its kinetics is more rapid due to the shorter diffusion length of carbon. As a result, the untransformed residual austenite is more enriched with carbon and the volume fraction of residual austenite is reduced. In that case, the formation of acicular ferrite is inhibited (or strongly reduced) for two main reasons. The first one is that the volume fraction of the retained austenite which can subsequently transform into acicular ferrite is reduced. The second one is that an increase of carbon concentration in the retained austenite reduces the amount of acicular ferrite because of the reduction of the temperature at which the acicular ferrite nucleates (more driving force is necessary to permit the transformation) and also by reducing its growth rate [22]. It is certainly for the same reasons that an increase in the cooling rate favours the formation of acicular ferrite.

As a partial conclusion, this mechanism is supported by both our observations and our measurements of BI evolution, which show that a higher cooling rate and a bigger initial austenite grain size favour the formation of acicular ferrite which develops in a more random direction and not only along the Mn poor regions as allotriomorph ferrite.

One of the remaining questions is why acicular ferrite can develop in a more isotropic direction and can grow in the Mn rich regions as well as in the Mn poor regions. One could put forward the assumption that acicular ferrite grows by repeated nucleation of subunits by displacive transformation [23]. It is supported by the fact that acicular ferrite microstructure exhibits surface relief phenomena, indicating that the formation of ferrite plates from austenite involves an invariant plane strain with a shear component [24]. If such displacive mechanism takes place without any diffusion of carbon and substitutional alloying elements, one can understand that acicular ferrite can develop randomly whatever the Mn composition. Our study by EBSD clearly shows that acicular ferrite plates are crystallographically related to the parent austenite grain approximately by the KS orientation relationship. These observations do not constitute a proof that the transformation is purely displacive since we can imagine that the ferrite nuclei can be formed by a so-called sympathetic nucleation [25] and the transformation can be subsequently controlled by carbon diffusion. Anyway, similar to the bainite transformation, this topic leads to controversies. Indeed, calculations based on carbon diffusion and local equilibrium at the austenite/ferrite interface yield growth rates that are in agreement with the experimentally observed ones [26]. Therefore, the acicular ferrite could grow with a rate controlled by the carbon diffusion in austenite all the more so the temperature of the transformation is relatively high in our case. Another reason that can explain for the banded structure to become less pronounced is that the acicular ferrite grows in some specific directions imposed by the crystallography and not by the distribution of Mn composition. In addition, it was observed from in situ measurements that the acicular ferrite can have multiple growth rates: from a moderated growth rate to a very fast one [27]. The growth rate could be a key factor since one could imagine a competition between the local transformation rate and the segregation rate. Indeed, if the growth rate is high enough, acicular ferrite can develop through the Mn rich regions. Probably, it may be one of the reasons that can explain when decreasing the transformation temperature [10] or increasing the cooling rate, the banding structure becomes less pronounced. Indeed, in these cases the driving force is higher and the transformation rate becomes more rapid.

Another original result of the present work is that, for a given cooling rate, the distance between the segregated bands—when existing—is reduced with decreasing the austenitization temperature or the austenite grain size (Figs. 11, 12, 13). This observation could be explained by considering that the initial Mn segregation shows less and more deep fluctuations, as can be visualized on the concentration map of Fig. 1b and schematized in Fig. 14.

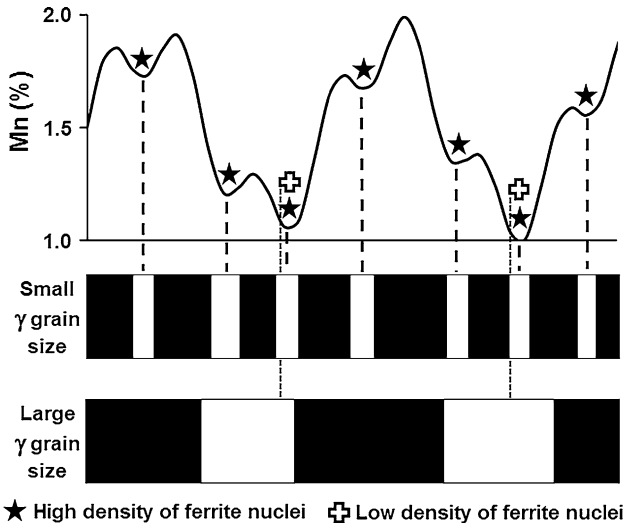

Fig. 14 Schematization of Mn segregation and microstructures expected to depend on the austenite grain size and the density of ferrite nuclei

These different levels of Mn segregation may be associated with the development of primary and secondary dendritic arms during solidification.

Thus, the influence of austenitization temperature T_γ could be understood through two different mechanisms that could act simultaneously:

(i) The first one is based on nucleation of ferrite. For low transformation driving forces, i.e. higher T_α or lower ρ_c, only deeper Mn valleys are expected to give rise to ferrite nuclei (white crosses in Fig. 14). In addition, allotriomorph ferrite is expected to be able to overcome lower Mn submits due to long distance carbon rejection. As a consequence, a coarser banded structure results. In case of slightly higher driving forces corresponding to lower ferritization temperatures, nucleation will be denser (black stars) and the carbon diffusion distance shorter, leading to finer microstructures. Higher T_γ temperatures coarsen the microstructure by smoothing the less deep Mn valleys.

(ii) The second one is based on the ferrite growth. Indeed, when the initial austenite grain size is bigger (the austenitization temperature is higher), the probability for Mn rich region to be intercepted by austenite grain boundaries is higher. Furthermore, the ferrite nucleates and grows rapidly along the austenite grain boundaries since the diffusivity of carbon is higher than the bulk diffusivity. As a consequence, ferrite can develop through the less deep Mn fluctuations. In that case, the Mn fluctuations are not efficient enough to slow down ferrite formation. As a result, the banding structure can be broken and reduced according to the evolution of BI given in Fig. 12. However, a coarser banded structure can be obtained.

It is necessary to perform a more complete study to decouple effects due to ferrite nucleation and those due to ferrite growth.

Conclusion

In this work, we proposed some new experimental data and their quantitative analysis, which clearly show that the ferrite transformation modes cannot be ignored in order to improve our understanding on the mechanisms of banding structure formation. Two types of ferrite—i.e. allotriomorph and acicular—are formed during the holding at a given temperature. These two transformation modes act differently on the segregated structure. The allotriomorph ferrite growths preferentially along the Mn poor regions and accentuates the banded structure. The acicular ferrite develops in more random directions from austenite grain boundaries and the resulting microstructure is more isotropic. The proposed mechanism is supported by both our observations and measurements of the BI index evolution. We have shown that the effects of the cooling rate and initial austenite grain size on the banding structure can be understood if one takes into account the effects of these parameters on the formation of the acicular ferrite.

Acknowledgements The authors gratefully acknowledge Region Lorraine and ArcelorMittal for the financial support of this work.

References

1. Samuels LE (1980) Optical microscopy of carbon steels. American Society for Metals, Ohio
2. Grostterlinden R, Kawalla R, Lotter U, Pircher H (1992) Steel Res 63:331
3. Bastien PG (1957) J Iron Steel Inst 187:281
4. Thompson SW, Howell PR (1992) Mater Sci Technol 8:777
5. Jatczak CF, Girardi DJ, Rowland ES (1956) Trans Am Soc Met 48:279
6. Verhoeven JD (2000) J Mater Eng Perform 9:286
7. Kirkaldy JS, Von Destinon-Forstmann J, Brigham RJ (1962) Can Metall Q 1:59
8. Offerman SE, Van Dijk NH, Rekveldt MT, Sietsma J, Van Der Zwaag S (2002) Mater Sci Technol 18:297
9. Xu W, Riviera-Del-Castillo PEJ, Van Der Zwaag S (2005) ISIJ Int 45:380
10. Krebs B (2009) PhD thesis, Université Paul-Verlaine de Metz
11. Krebs B, Germain L, Gouné M, Hazotte A (2011) Int J Mater Res 2:200
12. Serra J (1982) Image analysis and mathematical morphology. Academic Press, London
13. Stoyan D, Kendall WS, Mecke J (1987) Stochastic geometry and its applications. Wiley, New York
14. Schwarzer RA (1993) Textures Microstruct 20:7
15. Kurdjumov G, Sachs G (1930) Z Phys 64:325
16. Humbert M, Blaineau P, Germain L, Gey N (2011) Scr Mater 64:114
17. Allain S, Gouné M, Bouaziz O, Kassir E, Jantzen J (2011) J Mater Sci 46:2764
18. Kim DW, Suh DW, Qin RS, Bhadeshia HKDH (2010) J Mater Sci 45:4126
19. Bodnar RL, Hansen SS (1994) Metall Mater Trans A 25:763
20. Krahe PR, Kinsman KR, Aaronson HI (1972) Acta Metall 20:1109
21. Aaronson HI, Eylon D, Cooke CM, Enomoto M, Frees FH (1989) Scr Metall 23:435
22. Jones SJ, Bhadeshia HKDH (1997) Acta Mater 45:2911
23. Bhadeshia HKDH (2001) Bainite in steels, 2nd edn. IOM Communication Ltd, London
24. Strangwood M, Bhadeshia HKDH (1987) In: Proceedings of the conference on advances in welding science and technology, Ohio, USA, ASM International, p 187
25. Aaronson HI, Spanos G, Masamura RA, Vardiman RG, Moon DW, Menon ESK, Hall MG (1995) Metall Mater Trans B 32:107
26. Loginova I, Agren J, Amberg G (2004) Acta Mater 52:4055
27. Phelan D, Stanford N, Dippenaar R (2005) Mater Sci Eng A 407:127